

Lasers in Manufacturing Conference 2021

## New strategies for joining aluminum alloys to steel by means of laser

Daniel Wallerstein<sup>a,\*</sup>, Antti Salminen<sup>b</sup>, Fernando Lusquiños<sup>a</sup>, Rafael Comesaña<sup>c</sup>,  
Jesús del Val<sup>a</sup>, Antonio Riveiro<sup>c</sup>, Aida Badaoui<sup>c</sup>, Juan Pou<sup>a</sup>

<sup>a</sup>LaserON research group, CINTECX, School of Engineering, University of Vigo, Lagoas-Marcosende, Vigo, E-36310, Spain

<sup>b</sup>Department of Mechanical and Materials Engineering, University of Turku, Turku, FI-20014, Finland

<sup>c</sup>Materials Engineering, Applied Mechanics and Construction Dpt., University of Vigo, EEI, Lagoas-Marcosende, Vigo, E-36310, Spain

---

### Abstract

Joining steel and aluminum is still a challenging task, mainly due to significant differences in their melting temperatures, expansion coefficients and thermal conductivity, and to the practically zero solubility of Fe in Al. This low solubility leads to formation of brittle intermetallic compounds (IMCs) at the interface between aluminum and steel, which can seriously deteriorate the mechanical properties of the joint. Laser welding is a very competitive process that provides high energy densities, which results in moderate heat input, allied to high productivity and flexibility. On the other hand, although this joining process has been successfully applied to join aluminum to steel, high complexity and costs still hamper the acceptance of the technology by the industry. In this article, recent developments and limitations of laser joining of aluminum alloys to steel are briefly reviewed. Then, a new approach to join aluminum to steel in butt joint configuration is introduced. Lastly, a detailed microstructural and mechanical characterization of the resulting joints is presented.

Keywords: Multi-material design; dissimilar joints; mechanical properties; intermetallic compounds

---

### 1. Introduction

Multi-material design is recognized as an interesting approach to achieve weight reduction (Sakundarini et al., 2013), and so it has become necessary to develop strategies to join dissimilar materials. Laser welding is a

---

\* Corresponding author.

E-mail address: jpou@uvigo.es.

very promising technique when it comes to join dissimilar materials, mainly due to the precise control of the heat input while maintaining high levels of productivity and flexibility.

Due to aluminum's lightweight and good formability (Bajaj et al., 2020), and to steel's affordability, high strength and toughness (Ashkenazi, 2019), these are unarguably the most important metals for engineering applications. Thus, it is not surprising that joining aluminum to steel attracts much interest of the modern industries.

On the other hand, despite the advantages provided by aluminum-steel dissimilar joints, joining these two materials together is very challenging, mainly to the inevitable formation of intermetallic compounds (IMCs) at the joints' interface (Zhang et al., 2014). These IMCs are much more brittle than the base materials, so their formation and growth must be carefully taken into consideration in order to achieve joints with proper mechanical performance.

According to (Agudo et al., 2007), formation and growth of IMCs are consequence of chemical reactions and interdiffusion between Fe and Al. Therefore, strategies to suppress IMC formation and growth in dissimilar joints have been commonly based on chemical modifications of weld metal, and on controlling the welding thermal cycles.

The present article aims to briefly review the state of the art of aluminum-steel joining by means of laser, showing some of the most successful strategies published so far. Additionally, a new approach consisting in the combination of Al-Si-based welding wire and powder will be presented, together with the microstructural and mechanical characterization of the resulting dissimilar butt joints.

## **2. Brief review of the current state of the art of aluminum-steel dissimilar laser joining**

Lap and butt joints are the most common joint types in lightweight design. In the context of joining, the former has the advantage of increasing mounting tolerances and of being easily clamped, while the latter usually results in higher mechanical strength due to complete penetration, although issues related to joint fit-up and preparation might be concerning. Unlike in lap joints, the contact area in butt joints is limited to the thickness of the sheets. Therefore, lap joints usually show higher contact areas than butt joints. The resulting higher bonding area strongly influences mechanical performance of the joints (Meco et al., 2017). Moreover, in aluminum-steel dissimilar lap joints, one has to choose whether to place aluminum or steel on top. This choice changes significantly the joining approach, as these two materials show very different thermophysical properties between each other, such as melting ranges, thermal conductivities, thermal expansion coefficients, not to mention laser absorptivity coefficients.

Although some successful approaches to lap join aluminum to steel involve steel melting, most of the joining approaches attempt to melt the aluminum while keeping the steel in the solid state. The diffusion rates, which are responsible for IMC formation and growth, are much lower if steel melting is avoided (Zhang et al., 2017). Thus, due to the characteristics of the resulting joints, this joining approach has been called welding-brazing (Dharmendra et al., 2011).

Suitable wettability of molten aluminum on solid steel is very important in order to obtain sound mechanical properties in dissimilar joints, as poor wettability potentially decreases the bonding area. Having this in mind, (Mathieu et al., 2006) firstly proposed a hot-wire configuration, and then in (Mathieu et al., 2007) they used an in-line dual-beam approach, which redistributed the energy input and resulted in improved weld geometry, wettability and mechanical performance. Recently, (Huang et al., 2021) highlighted that although higher heat inputs lead to better wettability, IMC layer usually thickens due to higher diffusion rates. Thus, the balance between weld geometry and microstructure has to be found for each particular application, as highlighted by (Lahdo et al., 2018).

A common approach to enlarge the bonding area in butt joints is to bevel the sheets. Although this extra preparation step increases total time and costs, several authors have obtained interesting improvements in mechanical performance by using beveled sheets. (Sun et al., 2016) compared the use of 30° and 45° bevel angles in steel sheets, joining them to 60°-beveled aluminum sheets, and found that although the 30° condition resulted in thicker IMC layer, the larger bonding area resulted in better mechanical performance than the 45° condition. Also, they reported local heterogeneities in IMC layer thickness: it got thicker in the regions closer to the laser heat source. (Li et al., 2018a) also studied different combinations of bevel angles in both aluminum and steel sheets, and found good mechanical properties with a 45° bevel angle in steel sheet and a 45°-beveled half-Y shape in aluminum side.

Combination of two beams was proposed by several authors aiming at improving the mechanical performance of dissimilar joints. These configurations usually lead to a wider weld pool, lowering the temperature gradients within it, improving wettability, and sometimes helping to prevent occurrence of welding imperfections. (Cui et al., 2018) proposed an in-line dual-beam configuration, and studied the influence of power distribution and distance between the two beams. By varying these two parameters, they obtained sound dissimilar joints, controlling formation of imperfections such as microcracks and pores. Later, (Yuan et al., 2019) also used a dual-beam configuration, but in their case one beam was positioned on steel surface and another on aluminum's. The authors observed a competitive effect when energy density was varied: although wettability was improved with high energy densities (which in turn improves mechanical performance), IMC layer became thicker (resulting in joint embrittlement). Thus, the authors had to find the balance between these two features in order to maximize joints strength. More recently, (Xia et al., 2020) compared the application of single, cross (or parallel) and in-line (or tandem) beams to butt-join aluminum to steel, and found that cross beams homogenized the temperature distribution of the weld pool, resulting in thin IMC layer and absence of porosity.

Chemical modifications to the weld metal are also a common strategy for controlling IMC formation and growth. Although this approach can be applied to both lap and butt joints, the use of filler metals is more common to the latter joint type, while the former is commonly joined autogenously. (Xia et al., 2018) compared three different filler metals (pure Al, Al-5%Si and Al-12%Si) and found that the Al-12%Si eutectic composition resulted in the thinnest IMC layer. Additionally, ternary Fe-Al-Si intermetallics were formed when the Si-containing wires were used, while only binary Fe-Al IMCs were present in the pure Al filler wire condition. They obtained joints with very good mechanical properties, yet all steel sheets involved in the study were beveled. More recently, non-conventional high-entropy powders were applied by (Liu et al., 2020) as filler metals, resulting in thin IMCs layers due to delayed nucleation of precipitates. In turn, (Ogura et al., 2020) proposed inserting a Ti interlayer between the sheets, and achieved significant reduction of porosity in the dissimilar joints, reaching sound mechanical performance.

Microstructural modifications obtained by application of external magnetic fields were the object of study for several authors. Using this technique, (Chen et al., 2016) achieved important reduction in the diffusion rates of both carbon and aluminum, resulting in reduced austenite grain size and IMC layer thickness. (Yan et al., 2019) also showed very interesting results by applying external magnetic fields: they managed to modify the cross-section of joints from cylindric to conic, to decrease the element segregation, to avoid cracking, and to refine the resulting microstructure of the dissimilar joints. Recently, (Yan et al., 2021) also managed to improve the wettability of aluminum on steel and to control IMC layer thickness.

There are some common trends to all joining approaches: it is well known that it is desirable to obtain a thin and homogeneous IMC layer, to maximize bonding area, and obviously to avoid formation of welding imperfections as much as possible. Although several authors have managed to achieve these goals, relative complex, expensive and/or time-consuming joining approaches were used. Therefore, laser welding is still not broadly accepted by the industry when it comes to joining aluminum to steel. In this sense, in the following

section we will introduce a relatively simple and affordable joining approach that has been successfully applied to butt-join aluminum to steel, resulting in satisfactory mechanical properties but still limiting complexity and costs.

### **3. A new approach to join aluminum to steel in butt configuration**

As exposed above, different strategies have been proposed to join aluminum to steel successfully. However, on the one hand, these joining approaches usually involve whether complex systems, dual beam configurations, beveling the sheets, or non-conventional filler materials. These approaches usually increase costs, fabrication time and difficulty of operation, resulting in limited acceptance by the industry. On the other hand, there are no general rules available to lead us to the best combination of parameters in a particular application. It has been reported by several authors that some competitive effects, such as wettability improvement versus IMC thickening, usually take place. Thus, the search for the optimal processing conditions is usually very time-consuming, and the parameters are commonly assessed individually. Further, it is well known that the IMC layer is the most important concern in dissimilar aluminum-steel joints, as the failure usually takes place within this brittle region. Limited comprehension of the relation between processing conditions and resulting intermetallic compounds is still concerning in the context of dissimilar welding. Particularly, we believe that accurate IMC characterization is essential for improving our understanding. However, IMC identification is usually carried out by using almost exclusively scanning electron microscopy (SEM) and energy dispersive X-Ray spectroscopy (EDS). Few research works have based IMC identification on X-ray diffraction (XRD), transmission electron microscopy (TEM), or diffraction-based techniques such as electron backscattered diffraction (EBSD) and TEM-based selected area diffraction (SAED).

Therefore, in the present study, we propose a relatively simple and affordable joining approach, based on standard single beam fiber laser system, and on the combination of standard Al-Si filler metals, to butt-join unbeveled sheets of aluminum to steel. Additionally, instead of assessing each welding parameter individually, we carried out a combined parameters assessment, in order to promote future transferability and repeatability. We tried to identify the most common welding imperfections that take place in dissimilar aluminum-steel joining, and we suggested ranges of combined parameters that would prevent formation of such imperfections. Lastly, in the present work we took extra care in thoroughly and unambiguously characterizing the IMC layer present in the dissimilar joints by using a combination of advanced characterization techniques. We expect that our methodology will result in a joining approach that could be easily applied to the industry, and we also hope that our work will contribute to the technical literature

#### *3.1. Materials and experimental methodology*

The materials employed to carry out the laser joining experiments were 1.6 mm-thick 6061 aluminum alloy and 1.5 mm-thick S235-JR steel. An unbeveled butt joint configuration was chosen in order to perform the welding-brazing runs in flat position. Sample preparation consisted in grinding the aluminum sheets manually with sandpaper, and the steel sheets with a flap disk, and finally cleaning them all with acetone. As filler metals, ER4043 (Al-5%Si) welding wire with 1.0 mm diameter and Al-12%Si spherical powder were used. The powder was applied to the samples by previously mixing it to Nocolok flux, which is a standard brazing flux composed of potassium fluoroaluminates, and isopropyl alcohol, and finally by applying this mixture evenly at the bottom, lateral and top surfaces of both aluminum and steel sheets.

The equipment used for the welding-brazing runs was an IPG YLR- 3000S Ytterbium fiber laser (1070 nm-wavelength, 3 kW-maximum power). Optic setup consisted of a BK7 collimating lens (70 mm focal distance) and a BK7 convergent lens (200 mm focal distance). The laser beam had a Gaussian profile with a BPP of 4.094 mm \*mrad, and it was tilted 10 degrees from the vertical in order to avoid damaging the optics due to back reflection. The shielding gas used was Argon, flowing at approx. 15 liters per minute, and a copper plate was used as removable backing.

In order to define the parameters window that would permit the formation of sound dissimilar joints and avoid formation of welding imperfections as much as possible, we considered three combined parameters: power density (the ratio between laser power and beam area at working surface); interaction time (the ratio between beam diameter and welding speed) (Ashby and Easterling, 1984); and specific point energy (laser power times interaction time) (Suder and Williams, 2012). As we sought for avoiding melting the steel, the laser beam was always pointed to the aluminum sheet, in such a way that an off-set distance (the distance from the center of the beam to the joining axis) is an important parameter. Therefore, we introduced a new combined parameter, which is applied concretely to dissimilar joining: the ratio between specific point energy and off-set distance. This new combined parameter helped us expressing the amount of heat input applied to the dissimilar joining zone, which directly influences IMC formation and growth. Additionally, we selected some imperfections-free joints in order to carry out a thorough microstructural and mechanical characterization.

Microstructural characterization was carried out by applying a combination of techniques: SEM, EDS, XRD, EBSD and TEM-based SAED. SEM used was a FEI Quanta 200, equipped with detectors of backscattered and secondary electrons, and EDS. XRD was carried out using a Bruker AXS D8 diffractometer with X-ray Co tube. EBSD analysis was carried out by using a Helios 600 Nanolab Dual Beam SEM, with a Nordlys HKL Channel 5 detector. In the same equipment, lamellae were extracted by focused ion beam (FIB) technique with a liquid Ga ion source. Finally, the lamellae were used for the TEM/SAED analysis, which was carried out in a JEOL JEM-1010 unit.

Mechanical characterization of the joints was consisted of tensile and nanoindentation hardness tests. A Walter + Bai LFV 25 servohydraulic testing machine was used to carry out the tensile tests, which were performed in samples extracted transversely relative to the joint axis. Finally, MTS NanoXP Nanoindenter was used to carry out the nanoindentation hardness tests, which revealed both hardness and modulus of elasticity of the IMC layer.

### *3.2. Results and discussion*

In the welding-brazing experiments, different laser parameters were varied and the resulting joints were visually assessed in order to identify some welding imperfections that could take place. Thus, in Table 1 we present the range of combined parameters that lead to avoiding such imperfections to occur. Laser power was varied between 1200 and 3000 W; welding speed from 5 to 35 mm/s; beam diameter from 1.5 to 2.0 mm; wire feed speed from 20 to 50 mm/s; and off-set distance from 0.5 to 2.0 mm.

Table 1. Ranges of values of combined parameters that avoid formation of welding imperfections, and the imperfections that would take place beyond the defined ranges.

Combined parameter	Power density (W/mm <sup>2</sup> )	Interaction time (ms)	Specific point energy (J)	Specific point energy / off-set distance (J/mm)
Min. recommended value	800	150	350	300
Max. recommended value	1000	200	400	500
Imperfection if below	No melting	Humping	No melting	No brazing
Imperfection if above	Burn through, excessive IMC growth	Burn through, excessive IMC growth	Burn through, excessive IMC growth	Steel melts

Once knowing the range of values of combined parameters that lead to imperfections-free dissimilar joints, we proceeded to characterize the joints generated within the imperfections-free welds.

Fig 1 shows the cross-section of a dissimilar joint and the corresponding IMC layer in three different regions. Also, an EDS analysis of the central region is shown for Fe, Al and Si elements.

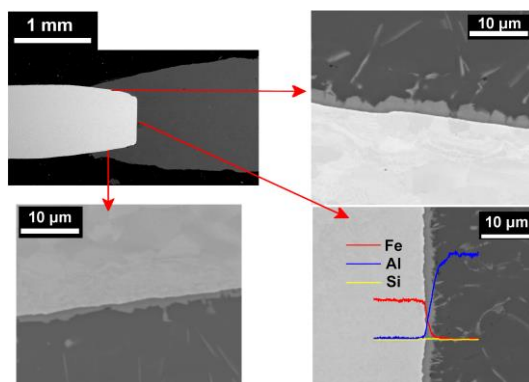


Fig. 1. Cross-section of a dissimilar joint, showing in detail the corresponding IMC layer in three different regions. The EDS analysis at central region is shown for Fe, Al and Si elements.

As one can see in Fig 1, the IMC layer is very thin ( $3 \pm 1 \mu\text{m}$ -thick) and considerably homogeneous throughout the joint cross-section. Additionally, the cross-section did not show any cracks or porosity. The appearance of the dissimilar joints is very satisfactory, considering that several authors reported local heterogeneities in the IMC layer of aluminum-steel joints, whether using Al-5%Si (Sun et al., 2016) or Al-12%Si welding wires (Li et al., 2018a, 2018b).

Continuing with the characterization of the joints, Fig 2 shows the XRD spectra of the dissimilar joints, in which we could identify the  $\text{Fe}_2\text{Al}_5$  and  $\text{Fe}_4\text{Al}_{13}$  binary intermetallics, and the  $\text{Fe}_4\text{Al}_{17.5}\text{Si}_{1.5}$  ternary intermetallic. As the intermetallic compounds are present in very small amounts in comparison to the base materials, some detailed regions of the complete spectra (Fig 2-a) are shown in Fig 2-b, -c and -d. In these detailed regions, some peaks that were difficult to identify in the complete spectra become more visible. In order to identify phases hidden by overlapping peaks in the spectra, Rietveld refinement technique was carried out by using Bruker AXS TOPAS analysis software.

$\text{Fe}_2\text{Al}_5$  and  $\text{Fe}_4\text{Al}_{13}$  are commonly seen in dissimilar aluminum-steel joints, whether the aluminum alloy belongs to 6xxx series (Cui et al., 2018; Xia et al., 2018; Xue et al., 2018) or to 5xxx (Chen et al., 2019; Qin et al., 2017). On the other hand, several authors have reported different ternary IMCs in dissimilar aluminum-steel joints, such as  $\text{Fe}_{1.8}\text{Al}_{7.2}\text{Si}$  (Qin et al., 2017; Song et al., 2009; Xia et al., 2020, 2019),  $\text{Fe}_2\text{Al}_8\text{Si}$  (Xia et al., 2018; Zhang et al., 2013), and  $\text{FeAl}_3\text{Si}$  (Zhang et al., 2017, 2016). However,  $\text{Fe}_4\text{Al}_{17.5}\text{Si}_{1.5}$  has never been reported in dissimilar joints obtained by fusion joining techniques before. In a metallurgic review article on the Fe-Al-Si ternary system, (Rivlin and Raynor, 1981) explained that  $\text{Fe}_4\text{Al}_{17.5}\text{Si}_{1.5}$  phase can take place in aluminum alloys showing 11 to 12%Si and 0.25 %Fe, cooling at rates higher than  $3^\circ\text{C}/\text{min}$ . These conditions are doubtlessly satisfied in the present work.

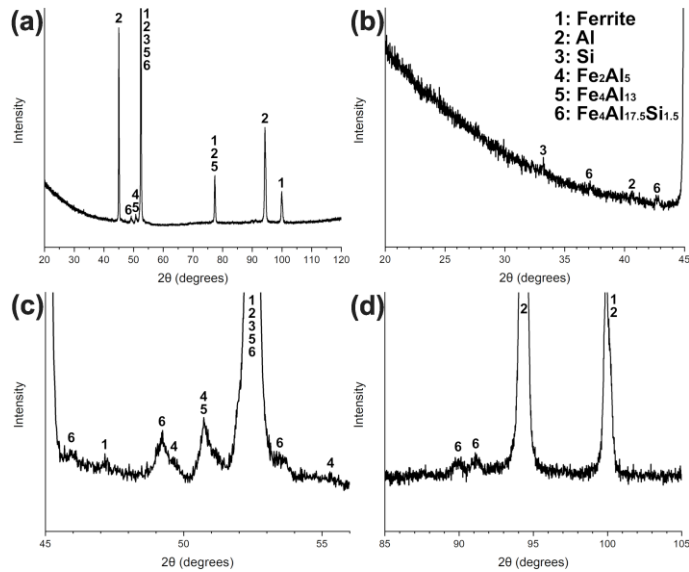


Fig. 2. (a) XRD spectra showing  $2\theta$  angle from  $20^\circ$  to  $120^\circ$ ; and detailed regions of the spectra showing  $2\theta$  from (b)  $20^\circ$  to  $45^\circ$ ; (c)  $45^\circ$  to  $56^\circ$ ; and (d)  $85^\circ$  to  $105^\circ$  degrees.

Once knowing the phases present in the dissimilar joints, we carried out an EBSD analysis seeking for obtaining a phase map located at the joining zone. Fig 3 shows the resulting EBSD map.

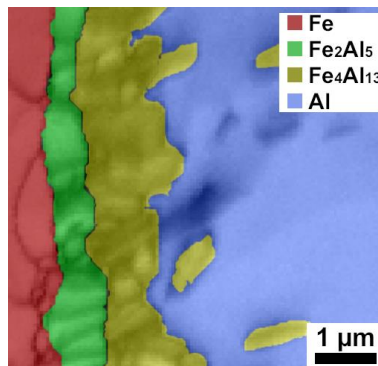


Fig. 3. Phase map obtained by EBSD showing the Fe and Al matrixes, and the binary  $\text{Fe}_2\text{Al}_5$  and  $\text{Fe}_4\text{Al}_{13}$  intermetallics.

As shown in Fig 3, besides the Fe and Al matrixes, we could locate the  $\text{Fe}_2\text{Al}_5$  and the  $\text{Fe}_4\text{Al}_{13}$  binary intermetallics. The former was found adjacent to the steel, while the latter is seen adjacent to the aluminum, as one should expect due to their stoichiometries. On the other hand, the ternary IMC identified by XRD was not detected by the EBSD. We believe that if the grain size of the ternary IMC is too small, its signal could be mixed with the signal from the Al matrix. To overcome this issue, we carried out a TEM-based SAED analysis, which is a more precise technique. With this technique, it is possible to assess small individual grains much more thoroughly. The results of the SAED analysis are shown in Fig 4. The SAED analysis could unambiguously confirm the presence of the  $\text{Fe}_4\text{Al}_{17.5}\text{Si}_{1.5}$  ternary IMC, which was present in very small grains.

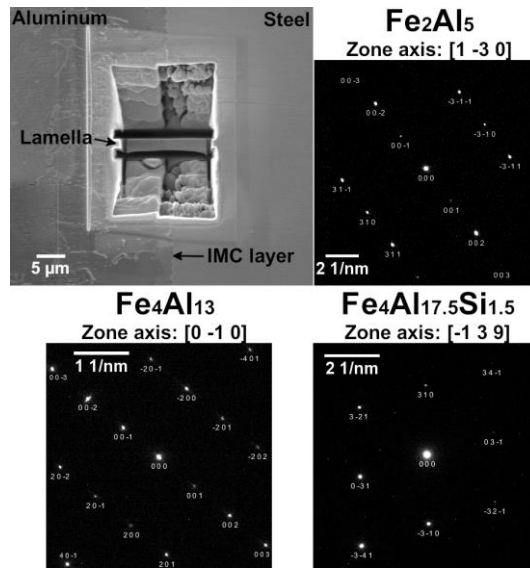


Fig. 4. Lamella extracted by FIB technique for the TEM/SAED analysis, and the resulting SAED patterns for the three IMCs.

Finally, the mechanical characterization of the joints was carried out by tensile and nanoindentation hardness tests. The summary of the mechanical properties encountered is shown in Table 2.

Table 2. Summary of the mechanical properties assessed in the study. The tensile test refers to the dissimilar joints, and the nanoindentation hardness test refers only to the IMC layer.

Mechanical tests	Mechanical properties	Values
Tensile test	Ultimate tensile strength	169 MPa
	Fracture strain	3.6 %
Nanoindentation hardness test	Hardness	$11.2 \pm 0.7$ GPa
	Modulus of elasticity	$257 \pm 24$ GPa



The mechanical properties shown in Table 2 reveal that although the ultimate tensile strength is satisfactory considering international standards, the fracture still presents a brittle behavior. The high values of hardness and modulus of elasticity presented by the IMC layer are responsible for the brittle behavior of the joint.

#### 4. Conclusions

In the first part of the article, recent successful approaches to join aluminum to steel are briefly reviewed. Due to its brittle behavior, the IMC layer is the most concerning region of dissimilar joints. Thus, regardless the joining strategy, controlling IMC formation and growth is usually the central issue. Several joining approaches presented in the review involve some relatively expensive systems and time-consuming steps, in reducing acceptance of the technique by the industry.

In the second part of the article, we present a new joining approach based on a standard fiber laser system, unbeveled butt joint configuration, and the combination of wire and powder as filler metals. We also present a combined parameters assessment that could be used to transfer the technology, and the resulting joints are microstructurally and mechanically characterized. Microstructural characterization revealed the presence of  $\text{Fe}_2\text{Al}_5$  and  $\text{Fe}_4\text{Al}_{13}$  binary IMCs, and of  $\text{Fe}_4\text{Al}_{17.5}\text{Si}_{1.5}$  ternary IMC. The mechanical characterization revealed that although the joints presented satisfactory strength, they still present a brittle behavior.

#### Acknowledgements

This work was partially supported by the Government of Spain (CDTI. CIEN: IDI-20150692), and by Xunta de Galicia (ED431C 2019/23, ED481A 2017/307, ED481D 2017/ 010, ED481B 2016/047-0). Authors would also like to acknowledge Prof. M.T. Pérez-Prado and Dr. X. Jin from IMDEA-Materials, and Prof. P. Adeva-Ramos and Dr. J.A. Jiménez from CENIM-CSIC for their cooperation on the characterization of the IMC layer. Additionally, we would like to acknowledge the technical staff from CACTI (University of Vigo).

#### References

- Agudo, L., Eyidi, D., Schmaranzer, C.H., Arenholz, E., Jank, N., Bruckner, J., Pyzalla, A.R., 2007. Intermetallic Fe x Al y -phases in a steel/Al-alloy fusion weld. *J. Mater. Sci.* 42, 4205–4214. <https://doi.org/10.1007/s10853-006-0644-0>
- Ashby, M.F., Easterling, K.E., 1984. The transformation hardening of steel surfaces by laser beams—I. Hypo-eutectoid steels. *Acta Metall.* 32, 1935–1948. [https://doi.org/10.1016/0001-6160\(84\)90175-5](https://doi.org/10.1016/0001-6160(84)90175-5)
- Ashkenazi, D., 2019. How aluminum changed the world: A metallurgical revolution through technological and cultural perspectives. *Technol. Forecast. Soc. Change* 143, 101–113. <https://doi.org/10.1016/j.techfore.2019.03.011>
- Bajaj, P., Hariharan, A., Kini, A., Kürsteiner, P., Raabe, D., Jägle, E.A., 2020. Steels in additive manufacturing: A review of their microstructure and properties. *Mater. Sci. Eng. A* 772, 138633. <https://doi.org/10.1016/j.msea.2019.138633>
- Chen, R., Wang, C., Jiang, P., Shao, X., Zhao, Z., Gao, Z., Yue, C., 2016. Effect of axial magnetic field in the laser beam welding of stainless steel to aluminum alloy. *Mater. Des.* 109, 146–152. <https://doi.org/10.1016/j.matdes.2016.07.064>
- Chen, S.S., Li, S., Li, Y., Huang, J., Chen, S.S., Yang, J., 2019. Butt welding-brazing of steel to aluminum by hybrid laser-CMT. *J. Mater. Process. Technol.* 272, 163–169. <https://doi.org/10.1016/j.jmatprotec.2019.05.018>
- Cui, L., Chen, B., Chen, L., He, D., 2018. Dual beam laser keyhole welding of steel/aluminum lapped joints. *J. Mater. Process. Technol.* 256, 87–97. <https://doi.org/10.1016/j.jmatprotec.2018.02.016>
- Dharmendra, C., Rao, K.P., Wilden, J., Reich, S., 2011. Study on laser welding-brazing of zinc coated steel to aluminum alloy with a zinc based filler. *Mater. Sci. Eng. A* 528, 1497–1503. <https://doi.org/10.1016/j.msea.2010.10.050>
- Huang, R., Tan, C., Sun, Y., Gong, X., Wu, L., Chen, B., Zhao, H., Song, X., 2021. Influence of processing window on laser welding-brazing of Al to press-hardened 22MnB5 steel. *Opt. Laser Technol.* 133, 106566. <https://doi.org/10.1016/j.optlastec.2020.106566>
- Lahdo, R., Springer, A., Meier, O., Kaierle, S., Overmeyer, L., 2018. Investigations on laser welding of dissimilar joints of steel and

- aluminum using a high-power diode laser. *J. Laser Appl.* 30, 032422. <https://doi.org/10.2351/1.5040643>
- Li, L., Xia, H., Tan, C., Ma, N., 2018a. Effect of groove shape on laser welding-brazing Al to steel. *J. Mater. Process. Technol.* 252, 573–581. <https://doi.org/10.1016/j.jmatprotec.2017.10.025>
- Li, L., Xia, H., Tan, C., Ma, N., 2018b. Influence of laser power on interfacial microstructure and mechanical properties of laser welded-brazed Al/steel dissimilar butted joint. *J. Manuf. Process.* 32, 160–174. <https://doi.org/10.1016/j.jmapro.2018.02.002>
- Liu, D., Wang, J., Xu, M., Jiao, H., Tang, Y., Li, D., Zhao, L., Han, S., 2020. Evaluation of dissimilar metal joining of aluminum alloy to stainless steel using the filler metals with a high-entropy design. *J. Manuf. Process.* 58, 500–509. <https://doi.org/10.1016/j.jmapro.2020.08.031>
- Mathieu, A., Pontevicci, S., Viala, J., Cicala, E., Mattei, S., Grevey, D., 2006. Laser brazing of a steel/aluminium assembly with hot filler wire (88% Al, 12% Si). *Mater. Sci. Eng. A* 435–436, 19–28. <https://doi.org/10.1016/j.msea.2006.07.099>
- Mathieu, A., Shabadi, R., Deschamps, A., Suery, M., Mattei, S., Grevey, D., Cicala, E., 2007. Dissimilar material joining using laser (aluminum to steel using zinc-based filler wire). *Opt. Laser Technol.* 39, 652–661. <https://doi.org/10.1016/j.optlastec.2005.08.014>
- Meco, S., Cozzolino, L., Ganguly, S., Williams, S., McPherson, N., 2017. Laser welding of steel to aluminium: Thermal modelling and joint strength analysis. *J. Mater. Process. Technol.* 247, 121–133. <https://doi.org/10.1016/j.jmatprotec.2017.04.002>
- Ogura, T., Wakazono, R., Yamashita, S., Saida, K., 2020. Dissimilar laser brazing of aluminum alloy and galvanized steel and defect control using interlayer. *Weld. World* 64, 697–706. <https://doi.org/10.1007/s40194-020-00858-7>
- Qin, G., Ji, Y., Ma, H., Ao, Z., 2017. Effect of modified flux on MIG arc brazing-fusion welding of aluminum alloy to steel butt joint. *J. Mater. Process. Technol.* 245, 115–121. <https://doi.org/10.1016/j.jmatprotec.2017.02.022>
- Rivlin, V.G., Raynor, G. V., 1981. 4: Critical evaluation of constitution of aluminium-iron-silicon system. *Int. Met. Rev.* 26, 133–152. <https://doi.org/10.1179/imtr.1981.26.1.133>
- Sakundarini, N., Taha, Z., Abdul-Rashid, S.H., Ghazila, R.A.R., 2013. Optimal multi-material selection for lightweight design of automotive body assembly incorporating recyclability. *Mater. Des.* 50, 846–857. <https://doi.org/10.1016/j.matdes.2013.03.085>
- Song, J.L., Lin, S.B., Yang, C.L., Fan, C.L., 2009. Effects of Si additions on intermetallic compound layer of aluminum–steel TIG welding–brazing joint. *J. Alloys Compd.* 488, 217–222. <https://doi.org/10.1016/j.jallcom.2009.08.084>
- Suder, W.J., Williams, S.W., 2012. Investigation of the effects of basic laser material interaction parameters in laser welding. *J. Laser Appl.* 24, 032009. <https://doi.org/10.2351/1.4728136>
- Sun, J., Yan, Q., Li, Z., Huang, J., 2016. Effect of bevel angle on microstructure and mechanical property of Al/steel butt joint using laser welding-brazing method. *Mater. Des.* 90, 468–477. <https://doi.org/10.1016/j.matdes.2015.10.154>
- Xia, H., Tao, W., Li, L., Tan, C., Zhang, K., Ma, N., 2020. Effect of laser beam models on laser welding–brazing Al to steel. *Opt. Laser Technol.* 122, 105845. <https://doi.org/10.1016/j.optlastec.2019.105845>
- Xia, H., Zhang, L., Tan, C., Wu, L., Chen, B., Li, L., 2019. Effect of heat input on a laser powder deposited Al/steel butt joint. *Opt. Laser Technol.* 111, 459–469. <https://doi.org/10.1016/j.optlastec.2018.10.032>
- Xia, H., Zhao, X., Tan, C., Chen, B., Song, X., Li, L., 2018. Effect of Si content on the interfacial reactions in laser welded-brazed Al/steel dissimilar butted joint. *J. Mater. Process. Technol.* 258, 9–21. <https://doi.org/10.1016/j.jmatprotec.2018.03.010>
- Xue, J., Li, Y., Chen, H., Zhu, Z., 2018. Wettability, microstructure and properties of 6061 aluminum alloy/304 stainless steel butt joint achieved by laser-metal inert-gas hybrid welding-brazing. *Trans. Nonferrous Met. Soc. China* 28, 1938–1946. [https://doi.org/10.1016/S1003-6326\(18\)64839-3](https://doi.org/10.1016/S1003-6326(18)64839-3)
- Yan, F., Wang, X., Chai, F., Ma, H., Tian, L., Du, X., Wang, C., Wang, W., 2019. Improvement of microstructure and performance for steel/Al welds produced by magnetic field assisted laser welding. *Opt. Laser Technol.* 113, 164–170. <https://doi.org/10.1016/j.optlastec.2018.12.030>
- Yan, F., Zhang, K., Yang, B., Chen, Z., Zhu, Z., Wang, C., 2021. Interface characteristics and reaction mechanism of steel/Al welds produced by magnetic field assisted laser welding-brazing. *Opt. Laser Technol.* 138, 106843. <https://doi.org/10.1016/j.optlastec.2020.106843>
- Yuan, R., Deng, S., Cui, H., Chen, Y., Lu, F., 2019. Interface characterization and mechanical properties of dual beam laser welding-brazing Al/steel dissimilar metals. *J. Manuf. Process.* 40, 37–45. <https://doi.org/10.1016/j.jmapro.2019.03.005>

- Zhang, M.J., Chen, G.Y., Zhang, Y., Wu, K.R., 2013. Research on microstructure and mechanical properties of laser keyhole welding–brazing of automotive galvanized steel to aluminum alloy. *Mater. Des.* 45, 24–30. <https://doi.org/10.1016/j.matdes.2012.09.023>
- Zhang, W., Sun, D., Han, L., Liu, D., 2014. Interfacial microstructure and mechanical property of resistance spot welded joint of high strength steel and aluminium alloy with 4047 AlSi12 interlayer. *Mater. Des.* 57, 186–194. <https://doi.org/10.1016/j.matdes.2013.12.045>
- Zhang, Y., Guo, G., Li, F., Wang, G., Wei, H., 2017. The interface control of butt joints in laser braze welding of aluminium-steel with coaxial powder feeding. *J. Mater. Process. Technol.* 246, 313–320. <https://doi.org/10.1016/j.jmatprotec.2017.03.020>
- Zhang, Y., Li, F., Guo, G., Wang, G., Wei, H., 2016. Effects of different powders on the micro-gap laser welding-brazing of an aluminium-steel butt joint using a coaxial feeding method. *Mater. Des.* 109, 10–18. <https://doi.org/10.1016/j.matdes.2016.07.011>